Journal of the European Ceramic Society **12** (1993) 369–375

Residual Stress and Microcracking in SiC–MgO Composites

J. Luo & R. Stevens*
School of Materials, The University of Leeds, Leeds, UK, LS2 9JT

(Received 11 December 1992; revised version received 5 April 1993; accepted 1 June 1993)

Abstract

The level of residual stress in SiC-particle-reinforced MgO composites has been investigated using X-ray diffraction. The significant difference in thermal expansion coefficients between SiC and MgO has resulted in the high residual stress in the composites. The stress measured has been compared with the calculated value evaluated using a Modified Eshelby's Model. Good agreement was obtained at low volume fractions of SiC addition to the MgO. At high volume fractions of SiC (>25%) a significant difference between measured and calculated values was obtained. This deviation has been shown to arise as a consequence of microcracking, which developed in the composites to release high levels of residual stress. The microcracking postulated as the strain relief mechanism was observed using TEM and SEM.

Das Maß an Eigenspannung in SiC verstärkten MgO-Verbundwerkstoffen wurde mit Hilfe der Röntgenbeugung untersucht. Der signifikante Unterschied in den thermischen Ausdehnungskoeffizienten zwischen SiC und MgO resultierte in einer hohen Eigenspannung des Verbunds. Die gemessene Spannung wurde mit dem Wert verglichen, der sich bei der Berechnung nach einem modifizierten Eshelby-Modell ergibt. Bei kleinem SiC-Volumenanteil ergab sich eine gute Übereinstimmung. Bei hohen Volumenanteilen (>25%) ergab sich ein erheblicher Unterschied zwischen den gemessenen und berechneten Werten. Die Abweichung folgt, wie gezeigt werden konnte, aus der Bildung von Mikrorissen die im Verbundwerkstoff entstehen, um die hohen Spannungen abzubauen. Der als dehnungsvermindernder Mechanismus vorgeschlagene Prozeß der Mikrorißbildung konnte in TEM und SEM beobachtet werden.

Le niveau des contraintes résiduelles dans un MgO renforcé de particules de SiC a été étudié par diffraction des rayons X. La différence significative entre les coefficients de dilatation thermique de SiC et de MgO conduit à des contraintes résiduelles élevées dans les composites. La contrainte mesurée a été comparée avec une valeur calculée au départ d'un modèle d'Eshelby modifié. Une bonne concordance est obtenue pour des fractions volumiques faibles de SiC ajouté au MgO. Pour des fractions volumiques élevées (>25%), une différence significative est obtenue entre les mesures et les valeurs calculées. Cette déviation a été considérée comme une conséquence de la microfissuration qui se développe dans les composites pour relaxer les niveaux élevés de contrainte. La microfissuration, postulée en tant que mécanisme de déformation du relief, a été observée par MET et MEB.

1 Introduction

Residual stress invariably develops in both single phase and multiphase ceramic materials, often due to fabrication and machining. The residual stress caused by machining tends to reside in layers near to the surface. Residual stress generated during fabrication may be produced by one or more of several mechanisms. The residual stress caused by the mismatch of thermal expansion coefficients between the matrix and reinforcement is particularly important in ceramic composites, since it can reach levels that have a significant effect on the mechanical properties of composites, and in limiting cases generate microcracking. In such materials, the average residual stresses[1] in the matrix ($\langle\sigma_M\rangle$) and the reinforcing phase ($\langle\sigma_I\rangle$) are in equilibrium, in conjunction with the volume fraction of the reinforcing phase (f), according to the following equation:

$$(1-f)\langle\sigma_M\rangle + f\langle\sigma_I\rangle = 0 \qquad (1)$$

The average residual stress has been evaluated in particulate composites by means of a Modified

* To whom correspondence should be addressed.

Journal of the European Ceramic Society 0955-2219/93/$6.00

Eshelby's Model (MEM),[2,3] which related especially to the sintering temperature and to the difference in the thermal expansion coefficients of the matrix and reinforcement phase.

The residual stress can also be measured experimentally. Root *et al.*[4] used neutron diffraction as a technique to measure it in alumina–mullite composites. A more commonly used method is X-ray diffraction (XRD) which has been used to determine the residual stress in ceramic composites.[5,6] Noyan and Cohen[7] have produced a comprehensive review of the topic.

The composites investigated in the present work consist of a range of SiC particle reinforced MgO, where the volume fraction of the SiC has been systematically increased. The thermal expansion coefficient of SiC (6×10^{-6}) is much less than that of MgO (15×10^{-6}) and this considerable difference, in conjunction with a temperature change, results in the development of high values of residual stress. This in turn has a significant effect on the mechanical properties in these and nano-composites[8,9] of a similar configuration. Any microcracking found in such a composite can usually be directly related to the generation of residual stresses.

In this paper, we report measurements of the residual stress related to the volume fraction of SiC present in SiC-reinforced MgO composites by means of XRD. Such experimental results have been compared with the predicted residual stress calcalculated by the MEM method. The microstructure and microcracking which develops, shown to be present using transmission (TEM) and scanning electron microscopy (SEM), has been related to the residual stress.

2 Experimental Procedure

SiC-particle-reinforced MgO composites were fabricated using hot pressing. The fabrication procedure has been described in a previous paper.[10] After cutting and grinding of the hot-pressed discs, samples were carefully polished before measurement of residual stress. This finishing process was systematically carried out in a manner designed to minimise the introduction of further residual stress into the surface.

Figure 1 shows the technique used to measure the residual stress by XRD. The principle underlying the XRD method is based on the measurement of the interplanar spacing d, at various angles of incident beam tilt, ϕ and ψ, as shown in Fig. 1. The change in the interplanar spacing along the L_3 axis, from the spacing do without residual stress, $(d - d_0)$, is related to the residual stress in the S-coordinate system by[7]

$$\frac{d-d_0}{d_0} = \frac{1-\nu}{E}(\sigma_{11}\cos^2\phi + \sigma_{12}\sin 2\phi + \sigma_{22}\sin^2\phi - \sigma_{33})\sin^2\psi + \frac{1+\nu}{E}\sigma_{33} - \frac{\nu}{E}(\sigma_{11}+\sigma_{22}+\sigma_{33}) + \frac{1+\nu}{E}(\sigma_{13}\cos\phi + \sigma_{23}\phi)\sin 2\psi \quad (2)$$

where σ_{ij} is the residual stress, and ν and E are Poisson's ratio and Young's modulus, respectively.

XRD was carried out using CuKα at 40 kV and 20 mA ($K\alpha_1 = 0{\cdot}1541$ nm, $K\alpha_2 = 0{\cdot}1545$ nm). The slits have a 1° divergence. The characteristic diffraction peaks chosen to measure the residual stress are shown in Fig. 2, (420) for MgO and (300) for SiC. The *hkl* interplanar spacings are 0·0942 nm for MgO and 0·0890 nm for SiC, respectively. The 2θ incremental scanning step for the X-ray measurement is 0·005°.

The microstructure of the composites was examined in a Jeol 200CX TEM. Two kinds of TEM samples were chosen: one was of a sintered sample; the other was cut from a section near to the fracture surface, after testing to failure in bending. The thin sections of the samples were ground and polished to about 20 μm, then further reduced in thickness using

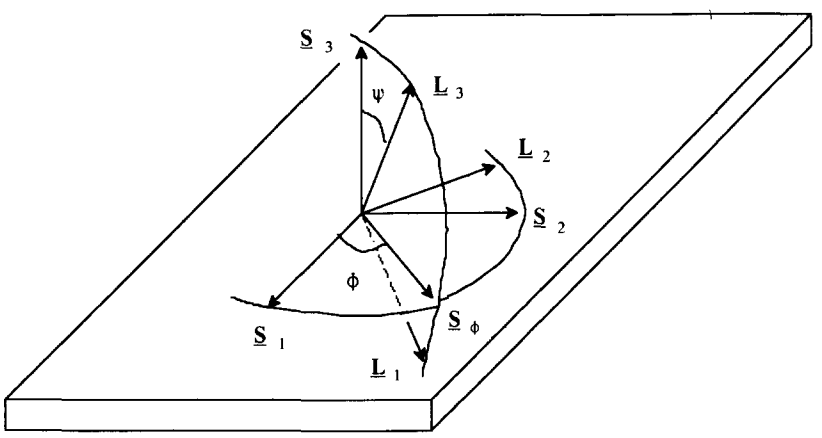

Fig. 1. Definition of the angles ϕ and ψ and the orientation of the laboratory coordinates L_i with respect to the sample coordinates S_i and the measurement direction S_ϕ.

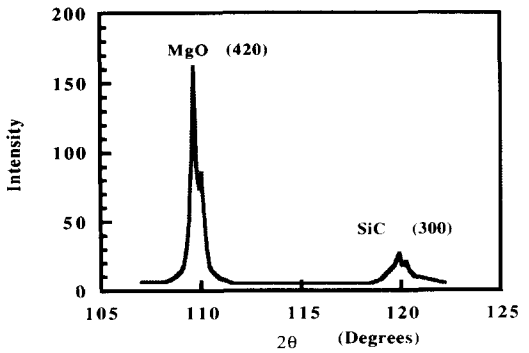

Fig. 2. X-Ray diffraction intensity peaks used for residual stress measurements of the MgO and SiC, respectively (20 vol% SiC–MgO).

an ion beam thinner, until a hole was observed in the centre of the sample. The polished and etched surface of the composite was observed using a Hitachi 700 SEM, after thermal etching in the range 1200–1300°C.

3 Experimental Results

Figure 3 shows the non-linear relationship between the change of interplanar spacing and $\sin^2\psi$. Such non-linearity indicates that a residual shear stress (σ_{13}, σ_{23}) exists on the surface, according to eqn (2). It is likely that this shear stress was introduced during the machining (grinding and polishing). Figure 3 also shows that the curves are affected by the rotation angles ϕ. For the two different angles 0° and 90°, eqn (2) can be rewritten as

$$\frac{d-d_0}{d_0} = \frac{1-\nu}{E}(\sigma_{11}-\sigma_{33})\sin^2\psi + \frac{1+\nu}{E}\sigma_{33} - \frac{\nu}{E}(\sigma_{11}+\sigma_{22}+\sigma_{33}) + \frac{1+\nu}{E}\sigma_{13}\sin 2\psi \qquad (\phi = 0^\circ) \quad (2a)$$

$$\frac{d-d_0}{d_0} = \frac{1-\nu}{E}(\sigma_{22}-\sigma_{33})\sin^2\psi + \frac{1+\nu}{E}\sigma_{33} - \frac{\nu}{E}(\sigma_{11}+\sigma_{22}+\sigma_{33}) + \frac{1+\nu}{E}\sigma_{23}\sin 2\psi \qquad (\phi = 90^\circ) \quad (2b)$$

For the composites, the average residual stress σ_1 should be the same as σ_2. The difference between σ_1 and σ_2 indicates that the fraction of the residual stress caused by the machining, i.e. the surface residual stress, is not neglected. The average values related to rotation ϕ between 0° and 90° were usually used to reduce the effect of inhomogeneous distribution of the stress caused by machining on the surface, also shown in Fig. 3. As the value of ψ

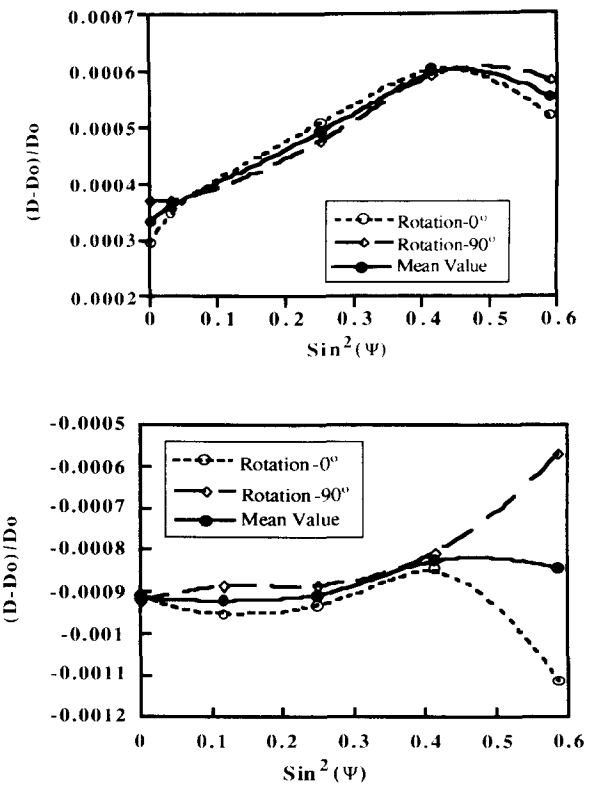

Fig. 3. Relationships between the change of interplanar spacing and $\sin^2(\psi)$.

increases, so the penetration depth of the X-ray beam into the surface of the materials decrease and the fraction of the surface residual stress attributed to machining will increase. Thus, the linear relationship between $\sin^2\psi$ and $(d-d_0)/d_0$ was used for values of the angle ψ less than 30°, to reduce the effect of the residual stress due to machining on the measurement of residual stress present in the bulk of the material due to thermal expansion mismatch.

For the present case, we ignore the effect of any shear stress (the last term for Eqn (2)). The mean curve (shown in Fig. 3) was chosen to represent a linear fit in order to calculate the residual stress using eqn (2). Figure 4, shows the residual stress obtained in relation to the volume fraction of SiC in the MgO. As can be seen from Fig. 3, the residual stress produced by machining (σ_{ij}^0) is sufficiently large that

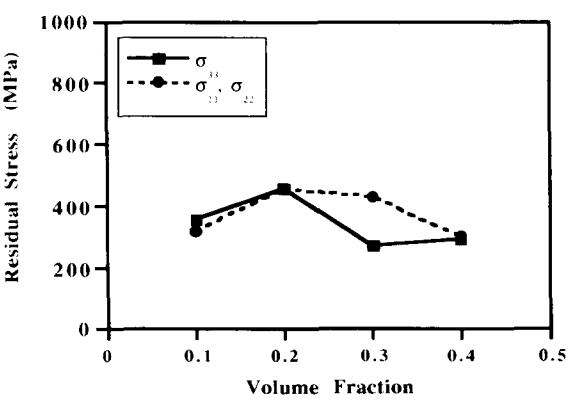

Fig. 4. The overall residual stress is the surface layer related to the volume fraction of SiC in the SiC-reinforced MgO.

it cannot be ignored. The relationships between the three kinds of stresses is as follows:[7]

$$\langle\sigma_{ij}\rangle_k^t = \sigma_{ij}^0 + \langle\sigma_{ij}\rangle_k^{pm}, \qquad (k = \mathrm{M}, \mathrm{I}) \qquad (3)$$

Subscripts M and I represent the matrix and reinforcement, respectively. $\langle\sigma_{ij}\rangle_{\mathrm{M}}^t$ and $\langle\sigma_{ij}\rangle_{\mathrm{I}}^t$ are the measured residual stresses. $\langle\sigma_{ij}\rangle_{\mathrm{M}}^{pm}$ and $\langle\sigma_{ij}\rangle_{\mathrm{I}}^{pm}$ are the residual stresses caused by the mismatch of thermal expansion coefficients between matrix and reinforcement. Combined with eqn (1), which expresses the relationship of the inner residual stress between matrix and reinforcement, the value of the inner residual stress was calculated by means of eqn (3) using the data measured by XRD (Fig. 4).

Figure 5 shows the internal residual stresses in both the MgO and SiC phases; each stress is caused by the mismatch of the thermal expansion coefficients. Compared with Fig. 4, the stress level is slightly different from that existing on the surface, except for the 20 vol% SiC composites, in which the overall residual stress in the MgO is much reduced below that calculated by mismatch of thermal expansion coefficients.

The theoretical residual stress, due to the mismatch of the thermal expansion coefficients between matrix and reinforcement, evaluated using the MEM[2,3] is also shown in Fig. 5. As can be seen, when the volume fraction of SiC particles is less than 20%, the measured residual stress is similar to the evaluation. As the volume fraction of SiC increases,

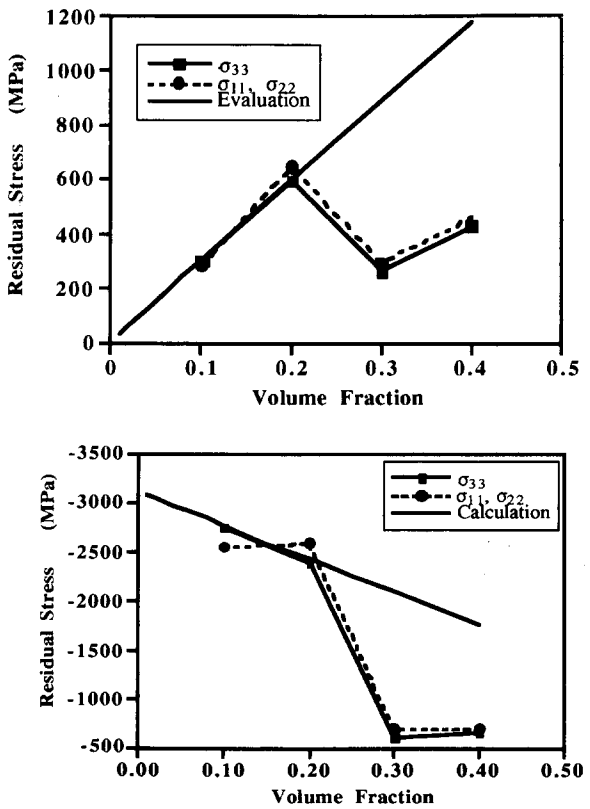

Fig. 5. The residual stress measured due to the mismatch of thermal expansion coefficients between SiC and MgO related to the volume fraction of SiC in SiC-reinforced MgO composites, compared with the evaluation by a MEM.

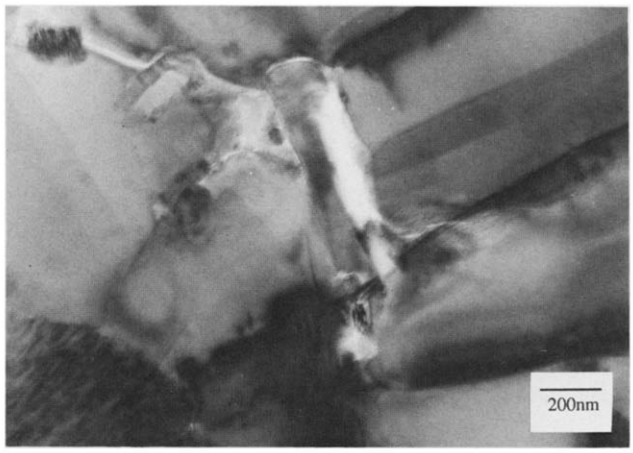

Fig. 6. Microstructure and microcracking in a 30 vol% SiC-reinforced MgO composite (TEM).

however, the experimental results deviate significantly from the theoretical values. There may be several factors which contribute to this difference. The microcracking in the MgO phase, which has been observed and will be discussed below, is possibly the most obvious factor to account for the deviation, since such microcracking will release considerable strain energy and hence reduce the level of the residual stress. The onset of extensive microcracking at a specific residual stress would then account for the abrupt deviation when the volume fraction of SiC is larger than 20 vol%.

3.1 Microstructure and microcracking

Figure 6 shows the microstructure of the SiC-particle-reinforced MgO composites observed using TEM (30 vol% SiC–MgO). Some microcracks were observed using TEM in the composites with 30 vol% and 40% SiC addition. The microcracking occurred in the MgO phase. No microcracking was observed in the 10% SiC-reinforced MgO composites. When the volume fraction of SiC is increased to 20% (Fig. 6), microcracking is present adjacent to the central hole of the thinned foil.

Figure 7 shows the microstructure of the 20%

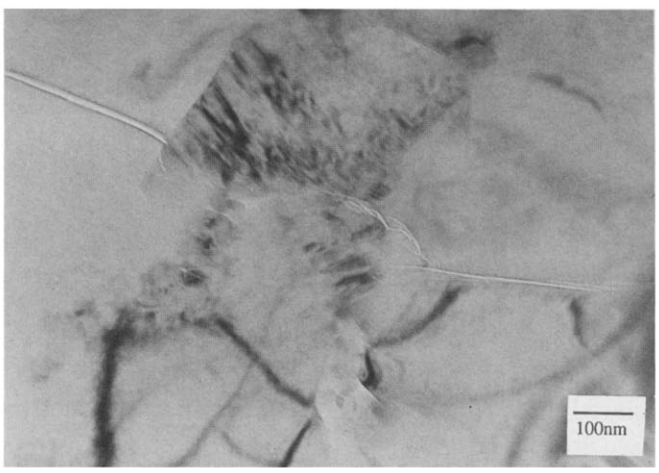

Fig. 7. Microcracking near the fracture surface in a 20 vol% SiC-reinforced MgO composite (TEM).

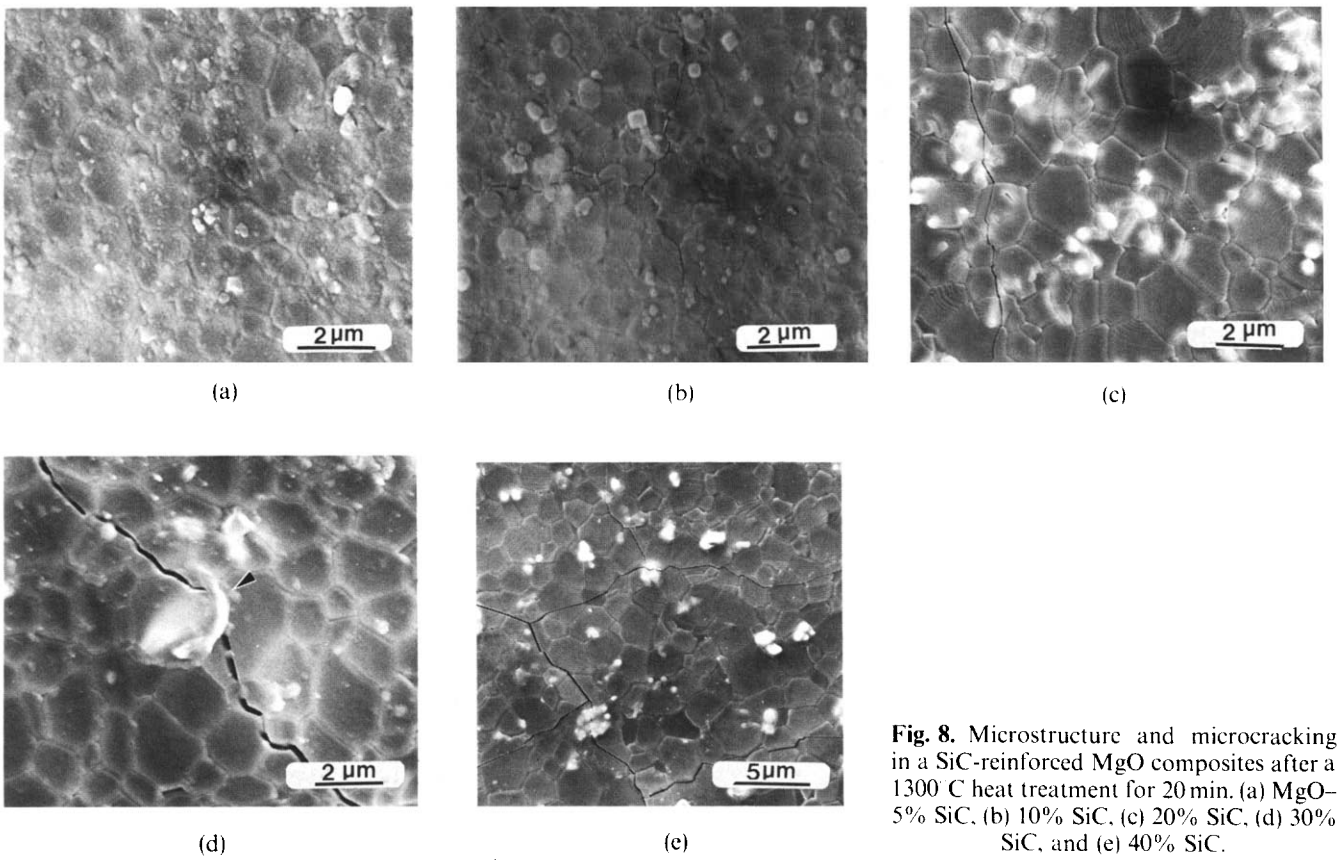

Fig. 8. Microstructure and microcracking in a SiC-reinforced MgO composites after a 1300°C heat treatment for 20 min. (a) MgO–5% SiC, (b) 10% SiC, (c) 20% SiC, (d) 30% SiC, and (e) 40% SiC.

SiC-reinforced MgO composite, for a sample cut near to the fracture surface, observed using TEM. In this case, extensive microcracking was readily observed, and the crack path usually passed through several grains of MgO. A possible explanation for such behaviour is that the microcracking which developed was due to not only the residual stress but to a combination of the bending stress and the stress generated during thinning and handling. It is apparent that the microcracking did not occur spontaneously, but was induced. Such induced microcracking is beneficial in that it can generate an effective increase in the fracture toughness of the composites.[10]

Figure 8 shows a micrograph of the polished surface of a composite after annealing, taken using SEM. Each composite was heat treated at a temperature of 1300°C for 20 min. Microcracks were observed in the MgO grains of all the composites with the exception of the 5 vol% SiC–MgO. The microcracks tend to be linked amongst the MgO grains. As the volume fraction of SiC increased, it became apparent that increasing numbers of MgO grains were found to exhibit microcracking and the opening displacement of the major cracks increased. As can be seen from Fig. 8, the crack propagation route passed through the MgO grains, i.e. transgranular cracking was taking place, in the process releasing the large residual stresses generated due to thermal expansion mismatch between the MgO and SiC. When the crack propagated towards or near to a SiC particle (Fig. 8(d)), the crack would tend to pass around the SiC particle. Subsequently, the SiC particle would become a bridge of the crack. For the composites made up of 10 vol% SiC, there were very few microcracks on the polished surface. Any microcracking observed was usually near regions with a high concentration of SiC particles, as shown in Fig. 8(b).

When the composites had been heated to 1300°C and immediately cooled, broadly similar results for the microcracking behaviour were observed, with the exception that the density of microcracking was reduced and the cracks were smaller, especially for the case of 10 vol% SiC, where the cracks became difficult to find.

When heated at 1200°C for 0·4 h, no microcracks were observed on the annealed surface of the 10 vol% SiC–MgO composites. Table 1 lists the grain size of the MgO after the composites had been

Table 1. The maximum grain size (μm) of the MgO component in the SiC-particle-reinforced MgO composites, after heat treatment

Annealing condition	*1300°C, 0·33 h*	*1300°C, 0·0 h*	*1200°C, 0·4 h*
5% SiC	~5	~3	—
10% SiC	~5	~3·5	~1·5
20% SiC	~5	~4	~2
30% SiC	~5	~4	~2
40% SiC	~5	~4	—

annealed for the three of heat treatment conditions. The MgO grain size is seen to have increased significantly above the original 1 μm size present before heat treatment, increasing with the temperature and holding time of the treatment.

4 Discussion

Microcracking of grains in ceramics takes place when the strain energy of a grain is equal to, or larger than, the critical strain energy (or fracture energy) for crack propagation. The critical grain size for microcracking is related to the fracture energy, γ, and the stress, σ, in the grain:[11-15]

$$bc = k\gamma/E\varepsilon^2 \quad (4)$$

where k is a constant and bc is the critical grain size for spontaneous microcracking; ε, is the residual strain present in the grains. The spontaneous microcracking of grains in SiC reinforced MgO composites is related to the grain size and the residual stress caused by the mismatch of thermal expansion coefficient. According to micromechanical analysis, the residual stress in MgO increases as the volume fraction of SiC increases, as shown in Fig. 5 evaluated by MEM. This gives a good estimate of the actual residual stress in the SiC–MgO composites before microcracking occurred. The residual stress or strain in the matrix,[2,3] shown in Fig. 4, can be related to the volume fraction of reinforcement. When the residual strain energy in MgO grains is equivalent to the fracture energy, then microcracking occurs in the grains. The critical grain size for microcracking for particles in particulate composites and polycrystalline ceramics, as expressed in eqn (4), was used to calculate the critical grain size for the matrix MgO of the MgO–SiC composites. The strain in eqn (4) was substituted by the residual strain in the MgO. Thus the critical grain size decreased as the volume fraction of SiC increased, as shown in Fig. 9.

The grain size of MgO is about 1·0 μm in the sintered composites. No spontaneous microcracking should occur in the composites according to the prediction made in Fig. 9. In fact, some microcracking was observed using TEM in the 30% SiC–MgO composites as well as in the 40% SiC–MgO composites (Fig. 6). That the residual stress measured is much less than was calculated by MEM (Fig. 5), can also be used as evidence that microcracking is taking place in both compositions. After the composites had been heat treated, the grain size increases, as listed in Table 1. Subsequently, more extensive microcracking was observed, even in the 10% SiC–MgO. Comparison of the appropriate grain size with the critical grain size predicted for microcracking, as shown in Fig. 9, shows the observed grain size for microcracking to be smaller than the calculated value, but that the trend for microcracking is similar, i.e. the degree of microcracking increases as the grain size of the MgO increases and the volume fraction of SiC increases.

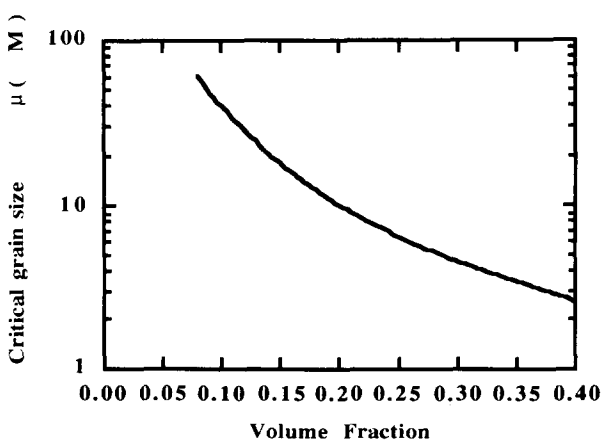

Fig. 9. The critical grain size for spontaneous microcracking related to the volume fraction of SiC, in SiC-particle-reinforced MgO composites.

The reasons for deviation of the onset of microcracking from the prediction conditions may be several. The residual stress due to machining, for example, exists in the finished surface, developed from the sample preparation as shown in Fig. 3. As a consequence, the microcracking on the surface (observed) should exhibit some degree of difference from that in the bulk of the sample. Another possible factor which could affect the microcracking is the distribution of SiC particles in the MgO. It is extremely difficult to fabricate composites with homogeneously distributed particles. In certain regions, the concentration of SiC can be much higher than the average volume fraction of SiC. In such localised regions, the residual tensile stress in the MgO will be increased above the average value (Fig. 5). Microcracking may then preferentially occur, even when the average residual stress and the grain size of MgO are much smaller than the predicted values. Such behaviour has been observed in heat-treated samples (Fig. 9). microcracking seen in the 10% SiC–MgO composites, for example, occurs in regions with the higher concentrations of SiC. Therefore, whereas the spontaneous microcracking occurs generally in 30 and 40 vol% SiC–MgO composites, the microcracking in lower volume fraction SiC composites is located in specific areas which are able to release residual stress (Fig. 5). This localised microcracking has a minimum effect in decreasing strength since it is less than the critical flaw size. On the other hand, the effect of releasing any residual tensile stress in the MgO as a consequence of microcracking is of benefit to the composites. The effect of the residual stress and microcracking on the mechanical properties (fracture toughness and rupture strength) has been discussed in a further paper.[10]

5 Conclusions

The residual stress in SiC-particle-reinforced MgO composites has been measured using XRD techniques. The large residual stress present in the ceramic is caused by the mismatch of thermal expansion coefficients between SiC and MgO. At a low volume fraction of SiC, it is found to be similar in value to that predicted by MEM. As would be expected, the predictions diverge from the measured values with the onset of microcracking. The differences of experimental and calculated results is shown to be mainly a consequence of microcracking, which has been observed using TEM and SEM.

Acknowledgements

The study was supported by the Chinese Government and the British Council. The authors would like to thank Mr D. Wright, Dr E. Gilbart, Mr A. Nichells and J. P. Harrington for their help and advice with experimental techniques.

References

1. Mori, T. & Tanaka, K., Average stress in matrix and average elastic energy of materials with misfitting inclusions. *Acta Metall.*, **21** (1973) 571–4.
2. Mura, T. (ed.), *Micromechanics of Defects in Solids*. Martinus, Nijhaff Publishers, The Hague, The Netherlands, 1982.
3. Luo, J. & Stevens, R., Thermal and mechanical stress fields in particulate composites (To be published).
4. Root, J. H., Sullivan, J. P. & Marple, B., Residual stress in alumina–mullite composites. *J. Am. Ceram. Soc.*, **74** (1991) 579–83.
5. Magley, D. J., Winholtz, R. A. & Kaber, K. T., Residual stresses in a two-phase microcracking ceramic. *J. Am. Ceram. Soc.*, **73** (1990) 1641–4.
6. Zhu, X. & Predecki, P., Comparison of residual stresses in hot pressed and sintered alumina silicon carbide composites. *Ceram. Engng. Sci. Proc.*, **12** (1991) 1574–85.
7. Noyan, I. C. & Cohen, J. B. (ed.), *Residual Stress—Measurement by Diffraction & Interpretation*. Springer-Verlag, New York, USA, 1987.
8. Niihara, K., *et al.*, Fabrication and properties of MgO–SiC nanocomposites. In *Proc. 1st Japan International SAMPLE Symposium*, 1989, pp. 1–6.
9. Yasuda, E., Bao, Q. & Niihara, K., The effect of fine SiC particles on the creep of MgO at high temperatures. *J. Am. Ceram. Soc.*, **100** (1992) 514–9.
10. Luo, J. & Stevens, R., Crack stopping mechanisms in SiC/MgO composites. *The Proceedings of the Pacific Rim International Conference on Advanced Materials and Processing*. TMS, Hangzhou, People's Republic of China, 1992.
11. Davidge, R. W., Cracking at grain boundaries in polycrystalline brittle materials. *Acta Metall.*, **29** (1981) 1695–702.
12. Avans, A. G. & Faber, K. T., Toughening of ceramics by circumferential microcracking. *J. Am. Ceram. Soc.*, **64** (1981) 394–8.
13. Avans, A. G., Microfracture from thermal expansion anisotropy: I single phase systems. *Acta Metall.*, **26** (1978) 1845.
14. Cleveland, J. J. & Bradt, R. C., Grain size/microcracking relations for pseudobrookite oxides. *J. Am. Ceram. Soc.*, **61** (1978) 478–81.
15. Rice, R. W. & Pohanka, R. C., Grain-size dependence of spontaneous cracking in ceramics. *J. Am. Ceram. Soc.*, **62** (1979) 559–63.